Enhancing the antimicrobial activity of alamethicin F50/5 by incorporating N-terminal hydrophobic triazole substituents.

Sanjit Das,[a] Khoubaib Ben Haj Salah,[a] Emmanuel Wenger,[b] Jean Martinez,[c] Jules Kotarba,[d] Vanessa Andreu,[d] Nicolas Ruiz,[e] Filippo Savini,[f] Lorenzo Stella,[f] Claude Didierjean,[b] Baptiste Legrand[c] and Nicolas Inguimbert*[a]

Abstract: We propose a simple and efficient strategy to significantly improve the antibacterial activity of peptaibols and other antimicrobial peptides by N-terminal capping with 1,2,3-triazole bearing various hydrophobic substituents on C-4. We showed, herein, that such N-terminal insertions on alamethicin F50/5 could enhance its antimicrobial activity on Gram-positive bacteria without modification of its overall three-dimensional structure. Indeed, while the native peptide and its analogues shared comparable helical contents, the crystal structure of one of the most active derivative showed a local slight distortion of the N-terminal extremity, which was also observed in solution using NMR spectroscopy. Importantly, fluorescence studies showed that the N-capped derivatives had increased affinity for liposomes, which may indicate they interacted more strongly with the bacterial membrane than alamethicin F50/5.

Introduction

The effectiveness of antibacterial chemotherapy is facing a tremendous challenge due to the emergence of high level resistance towards common antibiotics.[1] Antimicrobial peptides (AMPs) constitute an appealing alternative to traditional drugs as they first target the microbial membrane rapidly killing bacteria. For these reasons they are less likely to induce resistance compared to antibiotics targeting intracellular protein targets.[2] Indeed most AMPs act either by disrupting the bacterial membrane through the formation of channels or reach their intracellular targets after crossing the membrane. Even if the precise mechanism leading to cell death is not fully understood the primary event involves their association with the cell membrane.[3] Therefore, finding a way to reinforce this interaction could be of general interest for the development of AMPs and also of other classes of therapeutic peptides showing potential in the treatment of many diseases including cancer, cardiovascular, Alzheimer and immunity disorders, as well as for tumor targeting or medical imaging.[4],[5],[6] We propose a straightforward strategy to strengthen the peptide-membrane interaction without modifying the sequence of the AMPs via the single incorporation of highly hydrophobic moieties at their N-terminal extremity. Indeed, while sequence modifications could alter their three-dimensional structure and/or antimicrobial activity, N-terminal acylation or lipidation provide an alternative way tuning the peptide physicochemical properties while usually preserving the original sequences and biological activity.[7],[8],[9],[10] Furthermore, N-terminal acetylation, one of the most common peptide modifications, has been widely used for improving stability and bioavailability of therapeutic peptides, like for example the HIV cell entry inhibitor enfuvirtide, the gonatropin-releasing hormone antagonists abarelix and cetrorelix, the ADH-1 peptide applied for the treatment of malignant melanoma and the thymalfasin used for the treatment of viral hepatitis.[11], The N-terminal pyroglutamate constitutes a solution adopted for Lupron, used for treatment of advanced prostate cancer as well as for many other drug candidates that are currently in clinical trials.[12] In addition, in the case of Alamethicin F50/5 (Alm) the presence of the N-terminal acetylation, which increases its lypophilicity, might constitute a prerequisite for insertion into membranes. This is common to most peptaibols.[13] Nevertheless, N-terminal acetylases effectively remove the acetyl moiety promoting the action of amino-peptidases, thus leading to the peptide degradation. We propose a simple way to introduce various protease-resistant hydrophobic N-terminal capping on peptide sequences (fluorinated or trifluoromethylated phenyl, biphenyl, naphthyl, phenanthrenyl and pyrenyl moieties introduced at the C4 1,2,3-triazole position), which are expected to promote their interactions with the bacterial membrane, enhancing the AMP activity.[14] As a proof of concept, we chose Alm as a template to assess the impact of N-terminal modifications since its activity, three-dimensional structure and mechanism of action have been extensively studied.[15],[16] Alm is a twenty amino acid long peptaibol characterized by the presence of eight aminoisobutyric acid (Aib) residues, acetylated at the N-terminus and having a phenylalaninol residue at the C-terminus. Due to the presence of the non-proteinogenic amino acid Aib, Alm predominantly folds as an α-helix, is resistant to proteases and strongly binds to cell membranes.[17],[18],[19]

[a] S, Das, Dr, K, Ben Haj Salah, Pr, N, Inguimbert
USR 3278 CRIOBE
PSL Research University, EPHE-UPVD-CNRS, Université de Perpignan Via Domitia, Laboratoire d'Excellence « CORAIL »
Bâtiment T, 58 avenue P. Alduy, 66860 Perpignan, France.
E-mail: nicolas.inguimbert@univ-perp.fr

[b] Dr, E, Wenger, Pr, C, Didierjean
CRM2 (UMR UL-CNRS 7036) Faculté des Sciences et Technologies, Université de Lorraine
70239 Boulevard des Aiguillettes, 54506 Vandoeuvre-lès-Nancy, France.

[c] Pr, J, Martinez, Dr, B, Legrand
Institut des Biomolécules Max Mousseron (IBMM), UMR 5247 CNRS, Université de Montpellier,
15 avenue Charles Flahault, BP 14491, 34093 Montpellier Cedex 5.

[d] Dr.V. Andreu, J. Kotarba
Akinao, 58 avenue P. Alduy, 66860 Perpignan, (France).

[e] Dr, N, Ruiz
Laboratoire Mer Molécules Santé.
Université de Nantes, UFR de Sciences pharmaceutiques et biologiques
9 rue Bias - BP 61112, 44035 Nantes (France)

[f] F, Savini, Pr, L, Stella
Dipartimento di Scienze e Tecnologie Chimiche
Università di Roma
Tor Vergata Via della Ricerca Scientifica 00133 Roma Italy.

Supporting information for this article is given via a link at the end of the document.

Table 1. Sequence, and yields of alamethicin F50/5 **4a** and modified alamethicin **4b-7d**.

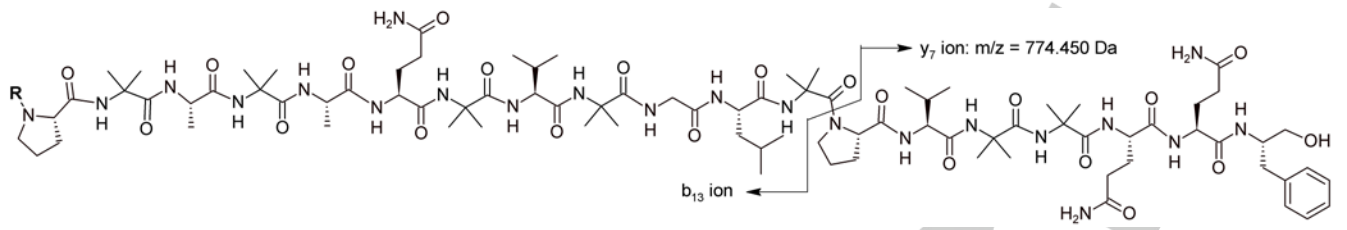

Compounds **4**			Compounds **5**			Compounds **6**			Compounds **7**		
	R	(%)[a]		R	(%)[a]		R	(%)[a]		R	(%)[a]
a	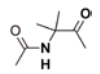	35	**a**	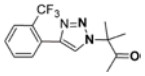	34	**a**	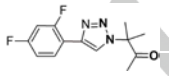	23	**a**	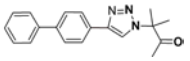	12
b	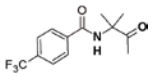	28	**b**	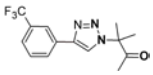	30	**b**	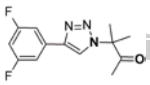	22	**b**	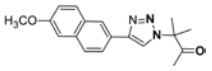	9
c	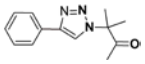	22	**c**	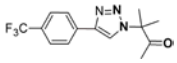	28	**c**	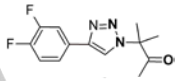	40	**c**	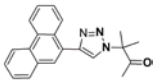	24
			d	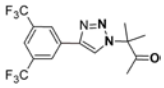	41	**d**	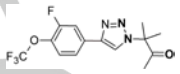	14	**d**	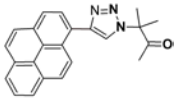	30

[a] Yields after semi preparative HPLC purification

These features confer to Alm its antimicrobial properties against Gram-positive bacteria with minimum inhibitory concentrations (MICs) ranging from 1.5 to 25 µM.[16] A wide array of techniques has been used to study Alm interactions with membranes.[20] In accordance with most reported studies, Alm first lies parallel to the membrane and tilts after reaching the threshold membrane-bound concentration, allowing insertion of the N-terminus into the bilayer, while the C-terminus remains exposed to the water phase.[21],[22] In the presence of a transmembrane potential, the peptide inserts more deeply into the bilayer, and self-associates, leading to the formation of barrel stave pores.[23] We have designed and synthesized novel Alm peptidomimetic analogues bearing 1,4-disubstituted-1,2,3-triazole (Tz) at their N-terminal part. We evaluated the antibacterial activity of these analogues, and using CD spectroscopy it was correlated to their structural changes. Importantly, we obtained the crystal structure of one N-capped derivative, which was also studied in the solution state using NMR spectroscopy. Finally, we performed fluorescence studies to assess the interaction between the analogues and liposomes as membrane models.

Results and Discussion

Compounds **3** contained a 1,4-disubstituted-1,2,3-triazole (Tz), substituents in position N-1 of Tz being analogous to the Aib in position 2 of the Alm sequence while position C-4 of Tz was decorated by aromatic groups of different nature, i.e. phenyl, fluorinated or trifluoromethylated phenyl, biphenyl, naphthyl, phenanthrenyl and pyrenyl moieties in order to increase Alm hydrophobicity (Scheme1, Table 1). The choice of these aromatic fragments results from their ability to accumulate into the lipid bilayer as a function of their lipophilicity, which can be advantageous to increase peptide interactions with the membrane.[24],[25] Furthermore, introduction of fluorinated moieties on the phenyl ring allowed to vary hydrophobicity without significantly increasing the overall fragment's size.[26],[27],[28] Recently, C-terminal fluorinated phenylalaninol was introduced in Alm using the biosynthetic machinery of *Trichoderma arundinaceum* without potency enhancement.[29] Compounds **3** were easily produced by copper azide-catalyzed cycloaddition between a commercially available ethynyl aromatic derivative **1** and 2-azido-2-methylpropanoic acid **2** issuing from a diazo transfert reaction applied to Aib (Scheme 1 and SI 2-22).[30],[31] Furthermore, compounds **3** were advantageous because they were ready to use for solid-phase peptide synthesis.

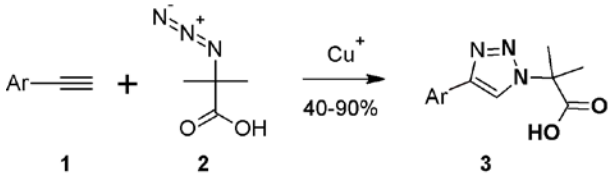

Scheme 1. Preparation of 1,4-disubstituted-1,2,3-triazole **3**.

The Alm derivatives containing a modified N-terminus were prepared using published synthetic protocols.[32],[33] Briefly, peptides were assembled by stepwise synthesis using Fmoc/tBu strategy on a chlorotrityl resin preloaded with phenylalaninol at a 0.1 mmol scale. Diisopropylcarbodiimide and oxymapure were used for 10 min coupling steps, and piperidine for Fmoc deprotection. All steps were performed under microwave, reaching a final temperature of 70°C.[34] Final deprotection with trifluoroacetic acid yielded peptides in satisfactory purity. Prior to biological assays, the compounds were purified by semi preparative HPLC to a final purity above 90%, and analyzed by LC/MS (Table1). As expected the pseudo molecular ion $[M+H]^+$ was not observed for compounds **4b**-**7** because of masses exceeding the m/z 2000 limit of the apparatus. Nevertheless, high intensity doubly charged ions $[M+2H]^{2+}$ and $[M+Na+H]^{2+}$ were observed along with y_7 and b_{13} diagnostic ions resulting from cleavage of the labile Aib13-Pro14 bond.[35],[36] More specifically, the y_7 ion with a m/z value of 774.45 Dalton was common to all the analyzed products while b_{13} m/z value varied according to the N-terminal modification (Table 1, SI 22-29). [37]

Table 2. Minimum inhibitory concentration (MIC) of alamethicin F50/5 **4a** and analogues **4b**-**7d**.

Cpd	MIC[a]	MIC[b]	IC_{50}[c]	$[\theta]_{220}$[d]	Helicity [e]
4a	12.5 ±6	12.5 ±6	18± 0.6	-12000	31
4b	12.5 ±6	*ND*	*ND*	-17300	44
4c	12.5 ±6	*ND*	6.3±1	-15100	39
5a	6.25 ± 0	*ND*	*ND*	-13000	34
5b	3.13 ± 3	*ND*	*ND*	-17000	44
5c	1.56 ±1,5	6.2 ± 0	2.9 ± 0.2	-16900	44
5d	3.13 ± 3	*ND*	*ND*	-14900	38
6a	3.13 ± 0	3.13 ± 0	3.9± 0.8	-14300	37
6b	3.13 ± 3	*ND*	*ND*	-14400	37
6c	3.13 ± 3	*ND*	*ND*	-14100	36
6d	3.13 ± 3	*ND*	*ND*	-16000	41
7a	3.13 ± 3	*ND*	*ND*	-15600	40
7b	3.13 ± 6	*ND*	*ND*	-17000	44
7c	1.56 ± 6	*ND*	*ND*	-14600	38
7d	1.56 ± 1,5	*ND*	*ND*	-15000	39

[a] µg/mL on *B. subtilis*. [b] µg/mL on *S. aureus*. [c] µg/mL on KB Cell. ND Not determined. [d] deg cm² $dmol^{-1}$. [e] %. Experiments performed in triplicate.

The antimicrobial activities of this peptide series were evaluated on *Bacillus subtilis*, *Staphylococcus aureus* (Table 2) and *Escherichia coli*. The Alm analogues having a N-terminal insertion were not potent against Gram-negative *E. coli* at 200 µM but retained and significantly enhanced their antimicrobial activity on Gram-positive targets such as *B. Subtilis* (Table 2) with minimal inhibitory concentrations (MIC) ranging from 1.56 to 12.5 µg/ml. The N-acetylated Alm **4a** and the Alm analogues bearing a fluorinated moiety bound to the sequence by a classical amide link **4b** and by a phenyl triazole **4c** exhibited the same antimicrobial activity on *Bacillus subtilis* (MIC 12.5 µg/mL). Such results indicated that hydrophobic N-capping groups linked by a peptide bond might not provide more potent derivatives than the N-acetylated native Alm. Also, a simple phenyl bore by a Tz might not be sufficiently hydrophobic to enhance its antimicrobial activity since all the other analogues with N-terminal "Tz-modifications" were more potent than Alm itself. Interestingly, compound **5c**, which had a trifluoromethyl moiety in para position of the phenyl linked to the Tz, was about eight times more potent (MIC 1.56 µg/mL) than Alm **4a** and compounds **4b** and **4c** (MIC 12.5 µg/mL for both of them). Moreover, in the series of compounds **5** substitution of the para position by a trifluoromethyl substituent led to a more active compound (**5c**, MIC 1.56 µg/mL) than when the substitution was in ortho position (**5a**, MIC 6.25 µg/mL) and meta (**5b**, MIC 3.13 µg/mL) positions. Introduction of two trifluoromethyl groups in meta position of the phenyl ring yielded compound **5d** as active as **5c** (MIC 3.13 µg/mL). Thus, comparing **4a** and **5c**, we noticed that the Tz seemed to have a role in the antimicrobial Alm activity increase.

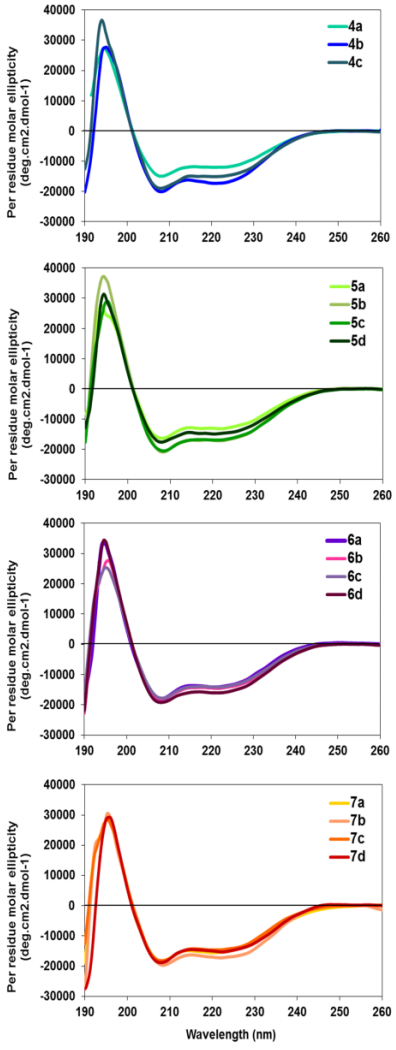

Figure 1. CD spectra of alamethicin F50/5 and its analogues (100µM) in methanol at 20°C.

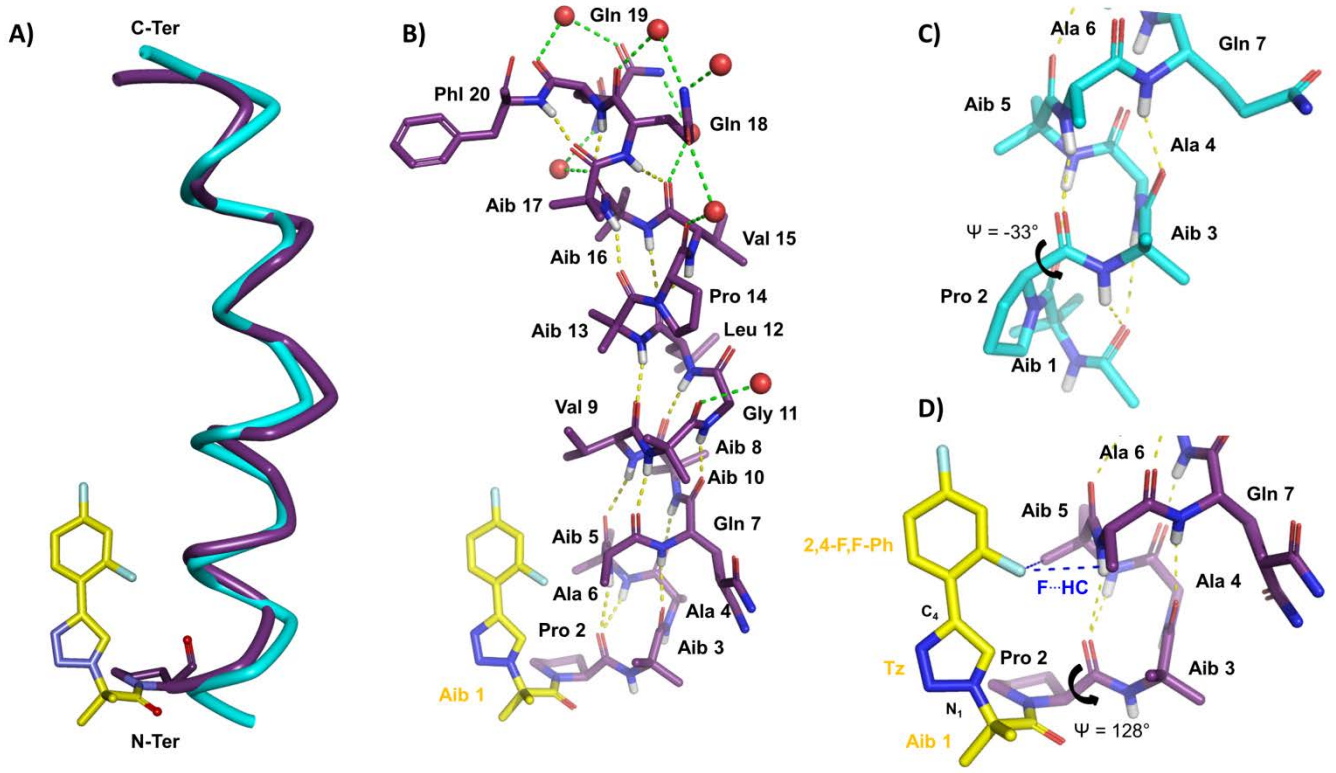

Figure 2. A) Backbone tube representation of the crystal structures of alamethicin (in cyan, PDB entry 1amt) and its analogue **6a** (in purple) triazole N-terminal capping is highlighted in yellow. B) Hydrogen bond network of the helix **6a**. Intramolecular hydrogen bonds and hydrogen bonds with water molecules are shown as yellow and green dotted sticks, respectively. Hydrogen atoms were omitted for clarity, except the amide protons. Water molecules located on the hydrophilic face are represented as red spheres. C and D) Comparison of the N-terminal parts of alamethicin **4a** and compound **6a**. The peculiar CH···F interactions between the N-capping and the side chains of Aib 5 and Ala 6 are represented as blue dotted sticks.

In contrast to **5**, compounds **6**, bearing two fluorine atoms at different positions of the phenyl ring, exhibited similar potency irrespective of the position of the substitutions (MIC 3.13 µg/mL), but they were all more efficient than Alm **4a**. Finally, for compounds **7**, containing polycyclic aromatic substituents of increasing size, the best antimicrobial activity on *B. subtilis* was obtained for compound **7d**, containing the bulky pyrenyl group (MIC 1.56 µg/mL). We then assessed the activity of two of the most active compounds **5c** and **6a** for further assays on *S. aureus* and on KB cell line deriving from a human carcinoma. The analogue **5c** was less active on *S. aureus* (MIC 6.2 µg/mL) than on *Bacillus subtilis*, but about twice more active than Alm. A comparable improvement of the antibacterial activity against *B. Subtilis* and *S. Aureus* (MIC = 3.13 µg/mL) was observed for **6a** (Table 2). We found that N-terminal insertions could also induce the growth inhibition of the KB cell line deriving from a human carcinoma growth, although peptaibols are known to be highly cytotoxic. Thus, we have demonstrated that various hydrophobic groups could be easily introduced via SPPS using pre-synthesized Tz-containing moieties to enhance the antimicrobial activities of Alm. The most active compounds were up to eight times more active than the native sequence. We then addressed the question if such N-modifications altered the structure of the Alm.

In order to evaluate if Alm derivatives **4b**-**7** retained the characteristic helical fold of peptaibols, we first examined their conformational preferences by using far ultra-violet circular dichroism (CD). Their CD spectra shared similar shapes typical of α-helical structures, with a maximum around 195 nm and two negative maxima of comparable intensity respectively centered at 208 and 225 nm (Figure 1). The helical content of the various compounds was rather close, between 31 and 40% (Table 2). The helicity percentage of the analogues was slightly higher than in Alm, which might suggest a weak stabilizing effect of the N-terminal hydrophobic tag. We cannot exclude an induced dichroism contribution of the absorbance of the aromatic moieties even if results show this effect is less significant than previously thought.[38],[39] Fortunately, we succeeded in crystallizing the analogue **6a** by slow evaporation in a methanol-water mixture. The asymmetric unit of **6a** contained one independent peptide chain. Residues 3-20 of compound **6a** showed a helical fold very close to those of the three independent wild-type Alm conformers, with a root mean square deviation values on Cα atoms of 1.0 ± 0.25 Å (PDB entry: 1AMT, Figure 2A, Tables S3).[15] Only the conformation of the two first residues were modified by the N-terminal addition of the 2,4-difluorophenyl triazole moiety, which induced a rotation of the ψ torsion angle of Pro 2 from about -33° to 128° (Figures 2C-D). Such alteration was driven by weak inter and intramolecular C-H···F interactions between the methyl group, the carbonyl of the Ala 7 and the fluorine atom in the *ortho* position of the 2,4-difluorophenyl (Figure 2D). These weak interactions were highlighted by Desiraju and co-workers from crystal structures of fluorobenzene derivatives.[40] The peculiar conformation of

the first three residues did not prevent a head-to-tail arrangement of the helices in the crystal, which were also observed in artificial helical architectures (Figure S1).[41],[42] The water molecules included in the structure formed hydrogen bonds with backbone carbonyls of Gly 11, Val 15, Aib 17 and the amide side chain of Gln 18 and 19, amino acids located on the hydrophilic face of the amphipathic alamethicin (Figure 2B).

NMR studies were performed on compounds **4a**, **5c** and **6a** in MeOH-d_3 at 298 K. We could assigned nearly all ^{1}H, ^{13}C and ^{15}N chemical shifts using homonuclear COSY, TOCSY, ROESY experiments and heteronuclear ^{15}N-HSQC, ^{13}C-HSQC, and ^{13}C-HMBC at natural abundance (Tables S4-S6). ^{3}J(HN,Hα) coupling constants (Table S7) and NOE cross-peaks were comparable for the three compounds and were consistent with a global helical shape in agreement with the CD signatures recorded for the whole compounds, the crystal structure of **6a** and the previous NMR structural studies on Alm.[43] As expected, the insertion of N-terminal capping locally modified the amide proton resonances especially in the N-terminal region, for both **6a** and **5c** (Figure S2). Thus, we controlled if the structural feature observed in the solid state for **6a** could also been observed in solution, but also if **5c**, which bore a different capping, exhibited a specific behaviour at its N-extremity. Based on the crystal structures of Alm and **6a**, we first identified diagnostic NOEs, which should allow to discriminate between the two conformers of the Pro 2 (ψ = -33° or 128°) and we monitored the putative long range NOEs between the capping and remote amino acids in the sequence (Figure S3). As expected for **4a**, we detected strong NOE peaks between 3.HN and 2.Hα-δ, and between the acetyl group and 3/4.HN, which were compatible with the helix turn of the Alm in this region (Figure S4). Unfortunately, strong overlaps prevented the accurate measure of the NOE volumes between the 3.HN and Pro 2 protons for **5c** and **6a** and the identification of the conformation of Pro 2. Nevertheless in **5c**, weak NOE correlations could be detected between the N-capping and Aib 3 while in **6a**, long range NOEs were observed with the Aib 5 and Ala 6 residues according to its structure in the solid state. In this context, incorporation of the fluorinated phenyl group via a Tz in **5c** apparently did not alter the N-terminal extremity of Alm, in contrast to the bifluorinated moiety in **6a**. Thus, depending on the nature of the capping, subsequent interactions, like C-H···F in the case of **6a**, could induce structural variations in the N-terminal region. Anyway, such feature did not turn off the activity of the derivatives (when we considered **6a**) and therefore it probably does not disturb neither their ability to self-assemble to form pores nor their interaction with the membrane. Such reorganization of the N-terminal part could be reversible close to the membrane and during oligomerization of the derivatives.

In this context, we chose to investigate the membrane interactions of **6a** and the highly active compound **7d** in comparison to Alm **4a.** We used the vesicle leakage assay to evaluate membrane permeabilization by the three compounds, using 5,6 carboxyfluorescein loaded liposomes (ePC/Chol 1:1) as previously described.[44]

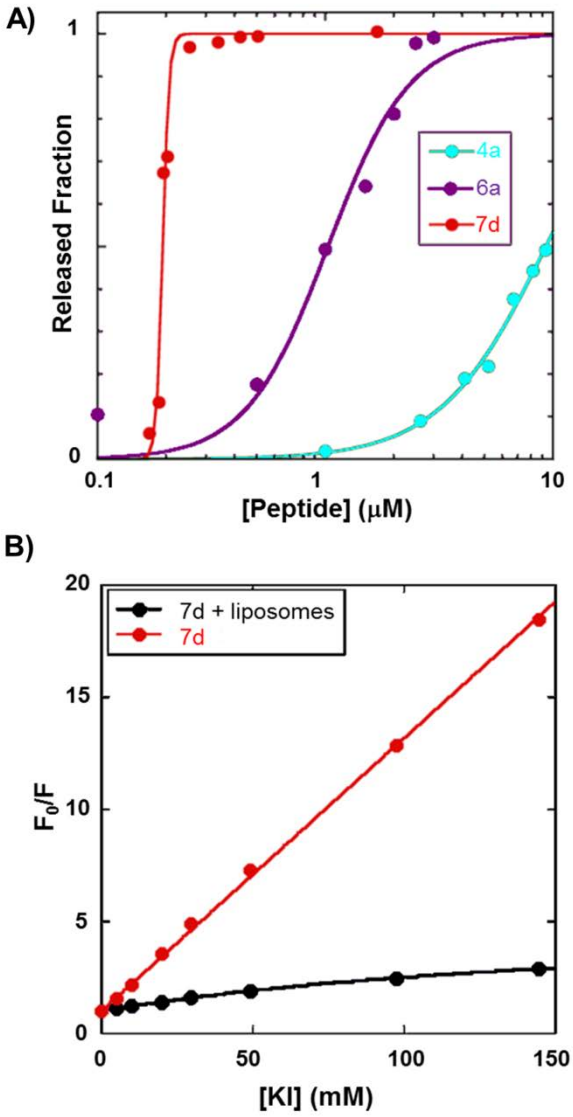

Figure 3. A) Fraction of liposome contents released 20 minutes after peptide addition. ePC/chol (1:1, mol/mol) liposomes, 100 nm diameter, [lipid] 20 μM. Data for Alm (**4a**) were taken as reference.[21] **B)** Stern-Volmer plot of KI quenching of **7d** (0.17 μM), free in solution and bound to liposomes; ePC/chol (1:1, mol/mol) liposomes, 100 nm diameter, [lipid] 100 μM.

Such technique is commonly used to measure the membrane activity of Alm and derivatives, and more generally of AMPs.[9],[21],[45] 5,6 carboxyfluorescein was encapsulated within lipid vesicles during liposome preparation. At high concentration, this fluorophore exhibits self-quenching limiting fluorescence emission. Upon pore formation, liposome leakage leads to the dilution of 5,6 carboxyfluorescein in the medium and

fluorescence emission increases.[44] Compounds **7d**, **6a** and **4a** released 50% of the fluorescent dye at concentrations of approximately 0.2, 1 and 10 μM concentration. In agreement with the antibacterial activity assays, **7d** and **6a** induced the release of the fluorescent dye from the liposomes at much lower concentrations than Alm (Figure 3A).[21] As expected, such results indicated that the primary target of the derivatives was the bacterial membrane like Alm. We also noticed a close relation between the potency of the compounds and their membrane permeation properties. At this stage, the higher activities of compounds **6a** and **7d** could be due to different reasons. They could form larger pores via different oligomerization states, self-assemble at lower concentrations and/or have higher affinities for the membrane. Next, we performed further investigations using the highly active compound **7d**. Interestingly, pyrenyl fluorescent moiety could be used to determine its self-assembly concentration and evaluate its affinity for membrane models. Indeed, the pyrene formed excited-state dimers (excimers) with a fluorescence spectrum well distinguished from that of the monomer.[46] Excimer formation is favored by the proximity of two pyrenyl moieties and is therefore indicative of aggregate formation.[47] Importantly, the excimer band at 475 nm appeared only at concentrations higher than 0.17 μM (Figure S5) indicating that **7d** started aggregating in buffer above this concentration, while no aggregation was detected by circular dichroism of Alm, up to a concentration of 100 μM.[21] We also showed that **7d** had a higher affinity for membranes than Alm by measuring the water/membrane partition by fluorescence. We determined for **7d** an apparent partition-constant of 150±10 10^5 at 0.17 μM, while a value of 1.4 10^5 had been previously reported for Alm at a higher peptide concentration of 6.7 μM (Figures S6 and S7).[21] Lastly, we examined the depth of insertion of the N-terminal part of **7d** in the membrane by measuring the fluorescence quenching of the pyrene by the iodide anion, which is unable to reach probes inserted in the hydrophobic core of the membrane.[43] As shown in Figure 3B, the pyrene fluorescence of the membrane-bound peptide was almost insensitive to potassium iodide quenching, demonstrating a deep insertion of **7d**. Thus, we have demonstrated that N-capped analogues could self-assemble and form pores at lower concentrations and exhibit better affinities for membrane models.

Conclusions

We have designed and synthesized a dozen of Alm analogues containing at the N-terminus a triazole ring substituted by aromatic moieties instead of the natural N-acetyl capping. These moieties were easily introduced by standard SPPS procedures and overcame limitations of conventional lipidation approaches such as incompatible reaction media or coupling and purification difficulties. Their introduction in Alm has led to analogues with increased antimicrobial activities, without significant alterations of the native peptide global structure even if slight variations depending on the nature of the inserted capping groups could be observed. Biophysical studies on selected compounds showed that the analogues could self-assemble at lower concentrations and had higher membrane affinities compared to Alm, probably due to increased hydrophobicity. We are currently preparing a library of capping moieties and expanding this strategy to various promising therapeutic peptides to enhance their activities but also to significantly increase their metabolic stability, half-life, and residence time in tissues. Importantly, we also showed that such strategy could be used to introduce various probes to study their mechanism of action, which might be useful also to track peptides in cells or small animals.

Experimental Section

Materials and Methods:

Reagents and solvents used in the synthetic process and for the chromatographic separation purpose were purchased from Sigma Aldrich Chemicals Ltd. (USA) and from Iris Biotech (Germany). Purifications of compounds **3** have been performed using column chromatography on silica gel (70-230 mesh and 63-200 μ particle size diameter). Thin layer chromatography was performed using different solvent mixtures based on the comparison of polarity of the desired compounds to be separated on pre-coated TLC sheets ALUGRAM SIL G/ UV254 (silica gel 60 F254 aluminium sheets from GmbH, Germany). Peptide were purified by semi-preparative HPLC using a Waters 1525 chromatography system with a Vydac 218MS510 column (250 x 10 mm) and fitted with a Waters 2487 tunable absorbance detector set to 214 nm and 254 nm. Purification was performed using 0.1% TFA in water (Buffer A) and 0.1% TFA in MeOH (0.1% TFA) (Buffer B) with a linear gradient A/B (20:80) to A /B (0:100) in 20 min at a flow rate of 2.5 mL/min. The nuclear magnetic resonance (NMR) spectra were taken for compounds **3** on a JEOL 400 DELTA spectrometer operating at 400 MHz field strength for 1H NMR and at 100 MHz for 13C NMR. LC-MS analysis was carried out using a Thermo Fisher Scientific liquid chromatography mass spectrometer, featuring an Accela HPLC coupled to a LCQ Fleet equipped with an electrospray ionization source and a 3D ion-trap analyser. MS spectra were recorded in positive mode. The analysis were performed with a Phenomenex Kinetex C-18 column (100 x 300 mm) using 0.1 % formic acid (FA) in water (Buffer A) and 0.1 % FA in methanol (Buffer B). Conditions of elution were: A/B (70:30) for 2 min followed by a linear gradient to A/B (0:100) in 20 min at a flow rate of 0.5 mL/min.

Synthesis of compound 3b-n:

Alkyne derivatives (5 mmol, 1eq.) were dissolved in 2 mL/mmol of t-BuOH/water (1:1). Then, Aib azide (5 mmol, 1 eq.) was added followed by copper sulphate (0.25 mmol, 0.05 eq.) and thereafter sodium ascorbate (0.5 mmol, 0.1 eq.) solution in 0.5 mL water were added into the reaction flask. The reaction mixture was stirred for 24 hr at room temperature. Progress of the reaction was monitored by

TLC. The mixture was concentrated and dissolved in the sufficient quantity of ethyl acetate and the organic layer was extracted 3 times with 1 M aqueous HCl solution. The organic layer was collected and dried over anhydrous magnesium sulphate, filtered and concentrated under reduced pressure. Crude products were purified by column chromatography using a mixture of cyclohexane and ethyl acetate.

Compound 3b: 820 mg (70.7 %), white amorphous solid, ^{1}H NMR (DMSO-d6): δ (ppm) 1.88 (6H, s), 7.32 (1H, t, J = 7.3 Hz), 7.45 (2H, t, J = 7.3 Hz), 7.88 (2H, d, J = 7.3 Hz), 8.78 (1H, s). ^{13}C NMR (DMSO-d6): δ (ppm) 25.8, 64.7, 121.1, 125.6, 128.3, 129.4, 131.4, 146.4, 173.5. MS (ESI+): calculated for $C_{12}H_{14}N_3O_2$ $[M+H]^+$ m/z 232.10; found m/z: 232.20.

Compound 3c: 880 mg (54.3%), white amorphous solid, ^{1}H NMR (DMSO-d6): δ (ppm) 1.89 (6H, s), 7.64 (1H, t, *J* = 7 Hz), 7.75 (2H, m), 7.86 (1H, d, J = 8 Hz), 8.43 (1H, s), ^{13}C NMR (DMSO-d6): δ (ppm) 25.8, 65.8, 123.6 (d, $^{3}J_{CF}$ = 3 Hz), 124.5 (q, $^{1}J_{CF}$ = 273 Hz), 126.9 (q, $^{3}J_{CF}$ = 5 Hz), 127.2 (q, $^{2}J_{CF}$ = 30 Hz), 129.4, 130.2, 132.5, 133.1, 143.8, 173.3. MS (ESI+): calculated for $C_{13}H_{13}F_3N_3O_2$ $[M+H]^+$ m/z 300.09; found m/z: 300.09.

Compound 3d: 560 mg (37.5%), white amorphous solid, 1H NMR(DMSO-d6): δ (ppm) 1.89 (6H, s) 7.70 (2H, m), 8.21 (2H, m), 9.02 (1H, s). ^{13}C NMR (DMSO-d6): δ (ppm) 25.7, 64.7, 122.0 (q, $^{4}J_{CF}$ = 3.9 Hz), 122.2, 124.7 (q, $^{1}J_{CF}$ = 272 Hz), 124.8 (q, $^{3}J_{CF}$ = 3.6 Hz), 129.3, 130.3 (q, $^{2}J_{CF}$ = 30 Hz), 130.7, 132.5, 145.0, 173.4. MS (ESI+): calculated for $C_{13}H_{13}F_3N_3O_2$ $[M+H]^+$ m/z 300.09; found m/z: 299.99.

Compound 3e: 645 mg, (43.2%), white amorphous solid, ^{1}H NMR (DMSO-d6): δ (ppm) 1.89 (6H, s), 7.82 (2H, d, *J* = 7.7 Hz), 8.11 (2H, d, *J* = 7.7 Hz), 8.99 (1H, s). ^{13}C NMR (DMSO-d6): δ (ppm): 25.9, 65.1, 122.6, 124.8 (q, $^{1}J_{CF}$ = 272 Hz), 126.1, 126.4 (d, $^{3}J_{CF}$ = 3.5 Hz), 128.4 (q, $^{2}J_{CF}$ = 32 Hz), 135.5, 144.9, 173.4. MS (ESI+): calculated for $C_{13}H_{13}F_3N_3O_2$ $[M+H]^+$ m/z 300.09; found m/z: 300.05.

Compound 3f: 874 mg (47.5%), white amorphous solid, ^{1}H NMR (DMSO-d6): δ (ppm) 1.91 (6H, s), 8.07 (1H, s), 8.55 (2H, s), 9.23 (1H, s). ^{13}C NMR (DMSO-d6): δ (ppm) 25.6, 64.9, 121.6 (m, $^{3}J_{CF}$ = 3.6 Hz), 123, 123.9 (q, $^{1}J_{CF}$ = 273 Hz), 125 (q, $^{3}J_{CF}$ = 2.5 Hz), 131.6 (q, $^{2}J_{CF}$ = 33 Hz), 133, 143.7, 173.2. MS (ESI+): calculated for $C_{14}H_{12}F_6N_3O_2$ $[M+H]^+$ m/z 368.08; found m/z: 368.06.

Compound 3g: 610 mg (45.4%), white amorphous solid, ^{1}H NMR (DMSO-d6): δ (ppm) 1.89 (3H, s), 7.22 (1H, td, *J* = 10 Hz, *J* = 2 Hz), 7.41 (1H, m, *J* = 10 Hz, *J* = 2 Hz), 8.12 (1H, q, *J* = 7 Hz), 8.51 (1H, d, *J* = 3 Hz). ^{13}C NMR (DMSO-d6): δ (ppm) 25.8, 64.9, 105.2 (t, $^{2}J_{CF}$ = 26 Hz), 112.3 (dd, $^{2}J_{CF}$ = 21.6 Hz, $^{4}J_{CF}$ = 3.4 Hz), 115.8 (dd, $^{2}J_{CF}$ = 13.7 Hz, $^{4}J_{CF}$ = 3.5 Hz), 129.4 (d, $^{4}J_{CF}$ = 4 Hz), 139.5 (d, $^{3}J_{CF}$ = 2.5 Hz), 159.1 (dd, $^{1}J_{CF}$ = 270 Hz, $^{3}J_{CF}$ = 11.7 Hz), 162.4 (dd, $^{1}J_{CF}$ = 247 Hz, $^{3}J_{CF}$ = 12 Hz), 173.4. MS (ESI+): calculated for $C_{12}H_{12}F_2N_3O_2$ $[M+H]^+$ m/z 268.09; found m/z: 268.05.

Compound 3h: 750 mg (56.1%), white amorphous solid, ^{1}H NMR (DMSO-*d*$_6$): δ (ppm) 1.88 (6H, s), 7.20 (1H, tt, *J* = 9.5 Hz, *J* = 2.3 Hz), 7.60 (2H, dt, *J* = 6.6 Hz, *J* = 2.3 Hz), 8.96 (1H, s). ^{13}C NMR (DMSO-*d*$_6$): *δ* (ppm) 25.7, 64.8, 103.6 (t, $^{2}J_{CF}$ = 25 Hz), 108.5 (dd, $^{2}J_{CF}$ = 19 Hz, $^{4}J_{CF}$ = 7 Hz), 122.7, 134.9 (t, $^{3}J_{CF}$ = 10 Hz), 144.5, 163.5 (dd, $^{1}J_{CF}$ = 231 Hz, $^{3}J_{CF}$ = 14 Hz), 173.3. MS (ESI$^+$): calculated for $C_{12}H_{12}F_2N_3O_2$ $[M+H]^+$ m/z 268.09; found m/z: 268.03.

Compound 3i: 720 mg (54%), white amorphous solid, ^{1}H NMR (DMSO-*d*$_6$): δ (ppm) 1.87 (6H, s), 7.52 (1H, qd, *J* = 8 Hz, *J* = 2 Hz), 7.74 (1H, m), 7.90 (1H, td, *J* = 10 Hz, *J* = 2 Hz), 8.86 (1H, s), ^{13}C NMR (DMSO-*d*$_6$): *δ* (ppm) 25.7, 64.7, 114.5 (d, $^{2}J_{CF}$ = 18 Hz), 118.8 (dd, $^{2}J_{CF}$ = 17 Hz), 121.8, 122.3 (dd, $^{3}J_{CF}$ = 6.4 Hz, $^{4}J_{CF}$ = 3 Hz), 144.6, 148.7 (dd, $^{1}J_{CF}$ = 245 Hz, $^{2}J_{CF}$ = 12 Hz), 150.4 (dd, $^{1}J_{CF}$ = 245 Hz, $^{2}J_{CF}$ = 12.9 Hz), 173.4. MS (ESI$^+$): calculated for $C_{12}H_{12}F_2N_3O_2$ $[M+H]^+$ m/z 268.09; found m/z: 268.19.

Compound 3j: 993 mg (59.5%), off-white amorphous solid, ^{1}H NMR (DMSO-*d*$_6$): δ (ppm) 1.9 (6H, s), 7.7 (1H, t, *J* = 8.0 Hz), 7.9 (1H, d, *J* = 8.8 Hz), 8.0 (1H, dd, *J* = 11.65 Hz, *J* = 2.07 Hz), 8.9 (1H, s). ^{13}C NMR (DMSO-*d*$_6$): *δ* (ppm) 25.7, 64.8, 114.3 (d, $^{2}J_{CF}$ = 20 Hz), 120.6 (d, $^{1}J_{CF}$ = 258 Hz), 122.4 (d, $^{3}J_{CF}$ = 3.5 Hz), 122.5, 125.3, 132.9 (d, $^{3}J_{CF}$ = 8 Hz), 134.9 (d, $^{2}J_{CF}$ = 13 Hz), 144.3, 154.5 (d, $^{1}J_{CF}$ = 250 Hz), 173.3. MS (ESI$^+$): calculated for $C_{13}H_{12}F_4N_3O_3$ $[M+H]^+$ m/z 334.08; found m/z: 334.04.

Compound 3k: 554 mg (36.0%), off-white amorphous solid, ^{1}H NMR (DMSO-*d*$_6$): δ (ppm) 1.90 (6H, s), 7.4 (1H, t, *J* = 7.3 Hz), 7.5 (2H, t, *J* = 7.6 Hz), 7.7 (2H, d, *J* = 7.3 Hz), 7.8 (2H, d, *J* = 8.4 Hz), 7.98 (2H, d, *J* = 8.4 Hz), 8.85 (1H, s). ^{13}C NMR (DMSO-*d*$_6$): *δ* (ppm) 25.8, 64.6, 121.3, 126.2, 127.1, 127.7, 128.1, 129.5, 130.5, 139.9, 140.1, 146.1, 173.5. MS (ESI$^+$): calculated for $C_{18}H_{18}N_3O_2$ $[M+H]^+$ m/z 308.14; found m/z: 308.18.

Compound 3l: 860 mg (55.4%), white amorphous solid, ^{1}H NMR (DMSO-*d*$_6$): δ (ppm) 1.9 (6H, s), 3.9 (3H, s), 7.2 (1H, dd, *J* = 9 Hz, *J* = 2.4 Hz), 7.3 (1H, d, *J* = 2.4 Hz), 7.9 (1H, d, *J* = 5.5 Hz), 8.0 (1H, dd, *J* = 9 Hz, *J* = 1.6 Hz) 8.3 (1H, s), 8.8 (1H, s). ^{13}C NMR (DMSO-*d*$_6$): *δ* (ppm) 25.8, 55.8, 64.7, 106.6, 119.7, 121.1, 123.8, 124.7, 126.7, 127.9, 129.1, 130.0, 134.4, 146.6, 158.0, 173.5. MS (ESI$^+$): calculated for $C_{17}H_{18}N_3O_3$ $[M+H]^+$ m/z 312.13; found m/z: 312.17.

Compound 3m: 1007 mg (60.7%), white amorphous solid, ^{1}H NMR (DMSO-*d*$_6$): δ (ppm) 2.0 (6H, s), 7.70 (4H, m), 8.0 (1H, dd, *J* = 7.8 Hz, *J* = 1.2 Hz), 8.1 (1H, s), 8.54 (1H, dd, 8.5 Hz, *J* = 1.1 Hz), 8.82 (1H, s), 8.88 (1H, d, *J* = 8.0 Hz), 8.94 (1H, d, *J* = 8.0 Hz). ^{13}C NMR (DMSO-*d*$_6$): *δ* (ppm) 25.9, 64.8, 123.4, 123.9, 124.1, 126.9, 127.3, 127.5, 127.6, 127.8, 127.9, 128.3, 129.3, 130.0, 130.2, 130.8, 131.5, 145.7, 173.5. MS (ESI$^+$): calculated for $C_{20}H_{18}N_3O_2$ $[M+H]^+$ m/z 332.14; found m/z: 332.21.

Compound 3n: 1767 mg (99.3%), bownish amorphous solid, ^{1}H NMR (DMSO-*d6*): δ (ppm) 1.9 (6H, s), 8.0 (1H, t, *J* = 7.6 Hz), 8.11 (1H, m), 8.2 (1H, s), 8.25 (2H, d, *J* = 9 Hz), 8.30 (2H, m), 8.35 (1H, s), 8.7 (1H, s), 9.0 (1H, d, J = 9.3 *Hz*). MS (ESI$^+$): calculated for $C_{22}H_{17}N_3O_2$ $[M+H]^+$ m/z 356.14; found m/z: 356.33.

Synthesis of compound 4-7:

SPPS was performed at 0.10 mmol scale on a CEM Liberty One microwave-assisted peptide synthesizer, for compounds (**4c**, **5c** and **6a**) and at 0.055 mmol for all other analogues using DIC/Oxyma as coupling reagent and 20% piperidine in DMF for deprotection of the Fmoc group. After transfer to the reaction vessel, the resin was swelled in DMF for 1h, then the elongation was carried automatically using 3-fold excess of each protected amino acid or compounds **3**, coupling reagents (0.3 mmol) under microwave irradiation at 70 °C for 20 min. Deprotection cycles were carried out with 20% piperidine in DMF (7 ml for 30s at 33 °C and 7 ml for 3 min at 70 °C). After completion of the synthesis, the peptidyl-resin was washed twice with 10 ml of DCM. Cleavage from the resin and complete deprotection were performed by treating the resin with 10 ml of

TFA/DCM/water/TIS 47:47:4:2 (v/v) for 60 min. The solution was sucked off, the filtrate was concentrated and co-evaporated with cyclohexane at a maximum temperature of 45°C. The peptide was precipitated with cold diethyl ether, recovered by centrifugation and washed with cold diethyl ether. The crude peptide was dissolved in water and freeze-dried prior to HPLC purification yielding a white product with purity above 95 %.

Compound 4a: Calculated for $C_{92}H_{151}N_{23}O_{24}$: $[M+H]^+$ m/z 1963.14 ; $[M+Na+H]^{2+}$ m/z 993.06 ; $[M+2H]^{2+}/2$ 982.06 ; $[M+3H]^{3+}$ m/z 655.05 ; b_{13} ion $[C_{55}H_{93}N_{14}O_{15}]^+$ 1189.69 ; y_7 ion $[C_{37}H_{60}N_9O_9]^+$ 774.45 ; found m/z: 1963.29 ; 993.02 ; 981.42 ; 655.08 ; 1189.35 ; 774.37.

Compound 4b: 32 mg (27.8 %). ESI^+ mass spectra: Calculated for $C_{98}H_{152}F_3N_{23}O_{24}$: $[M+H]^+$ m/z 2093.14 ; $[M+K+H]^{2+}$ m/z 1066.05 ; $[M+2Na]^{2+}$ m/z 1058.06 ; $[M+2H]^{2+}/2$ 1047.07 ; b_{13} ion $[C_{61}H_{94}F_3N_{14}O_{15}]^+$ 1319.70 ; y_7 ion $[C_{37}H_{60}N_9O_9]^+$ 774.45 ; found m/z: 1066.53 ; 1058.51 ; 1047.26 ; 1319.43 ; 774.47.

Compound 4c: 44 mg (21.5 %). ESI^+ mass spectra: Calculated for $C_{98}H_{153}N_{25}O_{23}$: $[M+H]^+$ m/z 2049.16 ; $[M+Na+H]^{2+}/2$ 1036.07 ; $[M+2H]^{2+}/2$ 1025.08 ; $[M+3H]^{3+}$ m/z 683.39 ; b_{13} ion $[C_{55}H_{93}N_{14}O_{15}]^+$ 1275.72 ; y_7 ion $[C_{37}H_{60}N_9O_9]^+$ 774.45 ; found m/z: 1036.25 ; 1024.39 ; 683.54 ; 1275.04 ; 774.27.

Compound 5a: 40 mg (34.4 %). ESI^+ mass spectra: Calculated for $C_{99}H_{152}F_3N_{25}O_{23}$ $[M+H]^+$ m/z 2117.15 ; $[M+K+H]^{2+}$ m/z 1078.05 ; $[M+Na+H]^{2+}$ m/z 1070.07 ; $[M+3H]^{3+}$ m/z 706.39 ; b_{13} ion $[C_{62}H_{94}F_3N_{16}O_{14}]^+$ 1343.70 ; y_7 ion $[C_{37}H_{60}N_9O_9]^+$ 774.45 ; found m/z: 1078.54 ; 1070.85 ; 706.43 ; 1343.49 ; 774.42.

Compound 5b: 35 mg (30.1 %). ESI^+ mass spectra: Calculated for $C_{99}H_{152}F_3N_{25}O_{23}$ $[M+H]^+$ m/z 2117.15 ; $[M+K+H]^{2+}$ m/z 1078.05 ; $[M+Na+H]^{2+}$ m/z 1070.07 ; $[M+3H]^{3+}$ m/z 706.39 b_{13} ion $[C_{62}H_{94}F_3N_{16}O_{14}]^+$ 1343.70; y_7 ion $[C_{37}H_{60}N_9O_9]^+$ 774.45 ; found m/z: 1078.50 ; 1070,81 ; 706.49 ; 1343.30 ; 774.36.

Compound 5c: 59 mg (27.9 %). ESI^+ mass spectra: Calculated for $C_{99}H_{152}F_3N_{25}O_{23}$ $[M+H]^+$ m/z 2117.15 ; $[M+2Na]^{2+}$ m/z 1081.07 ; $[M+Na+H]^{2+}$ m/z 1070.07 ; $[M+3H]^{3+}$ m/z 706.39 b_{13} ion $[C_{62}H_{94}F_3N_{16}O_{14}]^+$ 1343.70; y_7 ion $[C_{37}H_{60}N_9O_9]^+$ 774.45 ; found m/z: 1081.70; 1069,89 ; 706.42 ; 1343.12 ; 774.32.

Compound 5d: 50 mg (41.6 %). ESI^+ mass spectra: Calculated for $C_{100}H_{151}F_6N_{25}O_{23}$ $[M+H]^+$ m/z 2185.14; $[M+2Na]^{2+}$ m/z 1115.06 ; $[M+Na+H]^{2+}$ m/z 1104.06 ; $[M+2H]^{2+}/2$ 1093.07 ; b_{13} ion $[C_{63}H_{93}F_6N_{16}O_{14}]^+$ 1411.69 ; y_7 ion $[C_{37}H_{60}N_9O_9]^+$ 774.45 ; found m/z: 1115.58 ; 1104.32 ; 1093.50 ; 1411.45 ; 774.47.

Compound 6a: 49 mg (23.5 %). ESI^+ mass spectra: Calculated for $C_{98}H_{151}F_2N_{25}O_{23}$ $[M+H]^+$ m/z 2085.15 ; $[M+2Na]^{2+}/2$ = 1065.06 ; $[M+Na+H]^{2+}$ m/z 1054.06 ; $[M+2H]^{2+}/2$ 1043.07 ; $[M+3H]^{3+}$ m/z 695.72 b_{13} ion $[C_{61}H_{93}F_2N_{16}O_{14}]^+$ 1311.70; y_7 ion $[C_{37}H_{60}N_9O_9]^+$ 774.45 ; found m/z: 1065.34 ; 1054.03 ; 1042.92 ; 695.72 ; 1311.19 ; 774.34.

Compound 6b: 25 mg (21.81 %). ESI^+ mass spectra: Calculated for $C_{98}H_{151}F_2N_{25}O_{23}$ $[M+H]^+$ m/z 2085.15 ; $[M+K+H]^{2+}$ m/z 1062.05 ; $[M+Na+H]^{2+}$ m/z 1054.06 ; $[M+2H]^{2+}/2$ 1043.07 ; b_{13} ion $[C_{61}H_{93}F_2N_{16}O_{14}]^+$ 1311.70 ; y_7 ion $[C_{37}H_{60}N_9O_9]^+$ 774.45 ; found m/z: 1062.05 ; 1054.19; 1042.99 ; 1311.42 ; 774.50.

Compound 6c: 45 mg (39.3 %). ESI^+ mass spectra: Calculated for $C_{98}H_{151}F_2N_{25}O_{23}$ $[M+H]^+$ m/z 2085.15 ; $[M+Na+H]^{2+}$ m/z 1054.06 ; $[M+2H]^{2+}/2$ 1043.07 ; $[M+3H]^{3+}$ m/z 695.72 ; b_{13} ion $[C_{61}H_{93}F_2N_{16}O_{14}]^+$ 1311.70 ; y_7 ion $[C_{37}H_{60}N_9O_9]^+$ 774.45 ; found m/z: 1053.82 ; 1043.03 ; 696.34 ; 1311.41 ; 774.52.

Compound 6d: 16 mg (13.5 %). ESI^+ mass spectra: Calculated for $C_{99}H_{151}F_4N_{25}O_{24}$ $[M+H]^+$ m/z 2151.14 ; $[M+2Na]^{2+}$ m/z 1098.05 ; $[M+Na+H]^{2+}$ m/z 1087.06 ; $[M+2H]^{2+}/2$ 1076.07 ; b_{13} ion $[C_{62}H_{93}F_4N_{16}O_{15}]^+$ 1377.69 ; y_7 ion $[C_{37}H_{60}N_9O_9]^+$ 774.45 ; found m/z: 1098.59 ; 1087.03 ; 1076.26 ; 1377.35 ; 774.46.

Compound 7a: 14 mg (12 %). ESI^+ mass spectra: Calculated for $C_{104}H_{157}N_{25}O_{23}$ $[M+H]^+$ m/z 2125.20 ; $[M+2Na]^{2+}$ m/z 1085.08 ; $[M+Na+H]^{2+}$ m/z 1074.09 ; $[M+2H]^{2+}/2$ 1063.10 ; b_{13} ion $[C_{67}H_{99}N_{16}O_{14}]^+$ 1351.75 ; y_7 ion $[C_{37}H_{60}N_9O_9]^+$ 774.45 ; found m/z: 1085.83 ; 1074.08 ; 1063.44 ; 1351.40 ; 774.58 .

Compound 7b: 26 mg (9.2 %). ESI^+ mass spectra: Calculated for $C_{103}H_{157}N_{25}O_{24}$ $[M+H]^+$ m/z 2129.19 ; $[M+2Na]^{2+}$ m/z 1087.08 ; $[M+Na+H]^{2+}$ m/z 1076.09 ; $[M+2H]^{2+}/2$ 1065.09 ; $[M+3H]^{3+}$ m/z 710.40 ; b_{13} ion $[C_{66}H_{99}N_{16}O_{15}]^+$ 1355.74 ; y_7 ion $[C_{37}H_{60}N_9O_9]^+$ 774.45 ; found m/z: 1087.66 ; 1076.01 ; 1065.00 ; 710.48 ; 1355.40 ; 774.45.

Compound 7c: 28 mg (23.7 %). ESI^+ mass spectra: Calculated for $C_{106}H_{157}N_{25}O_{23}$ $[M+H]^+$ m/z 2149.19; $[M+Na+H]^{2+}$ m/z 1086.09 ; $[M+2H]^{2+}/2$ 1075.10 ; b_{13} ion $[C_{69}H_{99}N_{16}O_{14}]^+$ 1375.75 ; y_7 ion $[C_{37}H_{60}N_9O_9]^+$ 774.45 ; found m/z: 1086.20 ; 1075.98 ; 1375.59 ; 774.61.

Compound 7d: 35 mg (29.3%). ESI^+ mass spectra: Calculated for $C_{108}H_{157}N_{25}O_{23}$ $[M+H]^+$ m/z 2173.19 ; $[M+2Na]^{2+}$ m/z 1109.08 ; $[M+Na+H]^{2+}$ m/z 1098.09 ; $[M+2H]^{2+}/2$ 1087.10 ; $[M+3H]^{3+}$ m/z 725.07 ; b_{13} ion $[C_{71}H_{99}N_{16}O_{14}]^+$ 1399.75 ; y_7 ion $[C_{37}H_{60}N_9O_9]^+$ 774.45 ; found m/z: 1109.94 ; 1086.80 ; 725.60 ; 1399.37 ; 774.43 .

Acknowledgements

We thanks the “Bonus Qualité Recherche” of the university Perpignan Via Domitia, MESR, MIUR (grant PRIN 20157WW5EH_007) and Università di Roma “Tor Vergata” (Consolidate the Foundations grant AMPSA), for financial supports. The spectroscopic experiments have been performed at the “Laboratoire de mesures physiques” (LMP) at the university of Montpellier and using the “Biodiversité et Biotechnologies Marines” (Bio2Mar, http://bio2mar.obs-banyuls.fr/fr/index.html) facilities at the University of Perpignan. Grant of the GFPP allowing S Das internship in Pr Stella laboratory was appreciated. Access to the ‘Plateforme de mesures de diffraction X’’ of the Université de Lorraine was appreciated.

Keywords: Alamethicin F50/5 • 1,2,3-Triazole • Click Chemistry • α-helix • triazolopeptide

[1] M. F. Chellat, L. Raguž, R. Riedl, *Angew. Chem. Int. Ed.* **2016**, *55*, 6600–6626.
[2] A. T. Y. Yeung, S. L. Gellatly, R. E. W. Hancock, *Cell. Mol. Life Sci.* **2011**, *68*, 2161.
[3] W. C. Wimley, *ACS Chem. Biol.* **2010**, *5*, 905–917.
[4] A. K. Marr, W. J. Gooderham, R. E. Hancock, *Curr. Opin. Pharmacol.* **2006**, *6*, 468–472.

[5] A. F. G. Cicero, F. Fogacci, A. Colletti, *Br. J. Pharmacol.* **2017**, *174*, 1378–1394.
[6] S. Lien, H. B. Lowman, *Trends Biotechnol.* **2003**, *21*, 556–562.
[7] R. J. Wallace, *Br. J. Nutr.* **1992**, *68*, 365–372.
[8] L. Di, *AAPS J.* **2014**, *17*, 134–143.
[9] C. Toniolo, M. Crisma, F. Formaggio, C. Peggion, V. Monaco, C. Goulard, S. Rebuffat, B. Bodo, *J. Am. Chem. Soc.* **1996**, *118*, 4952–4958.
[10] E. Gatto, C. Mazzuca, L. Stella, M. Venanzi, C. Toniolo, B. Pispisa, *J. Phys. Chem. B* **2006**, *110*, 22813–22818.
[11] P. Vlieghe, V. Lisowski, J. Martinez, M. Khrestchatisky, *Drug Discov. Today* **2010**, *15*, 40–56.
[12] K. Fosgerau, T. Hoffmann, *Drug Discov. Today* **2015**, *20*, 122–128.
[13] N. Stoppacher, N. K. N. Neumann, L. Burgstaller, S. Zeilinger, T. Degenkolb, H. Brückner, R. Schuhmacher, *Chem. Biodivers.* **2013**, *10*, 734–743.
[14] N. C. Yoder, K. Kumar, *Chem. Soc. Rev.* **2002**, *31*, 335–341.
[15] R. O. Fox, F. M. Richards, *Nature* **1982**, *300*, 325–330.
[16] L. Kredics, A. Szekeres, D. Czifra, C. Vágvölgyi, B. Leitgeb, *Chem. Biodivers.* **2013**, *10*, 744–771.
[17] J. W. Payne, R. Jakes, B. S. Hartley, *Biochem. J.* **1970**, *117*, 757–766.
[18] H.-H. Nguyen, D. Imhof, M. Kronen, B. Schlegel, A. Härtl, U. Gräfe, L. Gera, S. Reissmann, *J. Med. Chem.* **2002**, *45*, 2781–2787.
[19] H. YAMAGUCHI, H. KODAMA, S. OSADA, F. KATO, M. JELOKHANI-NIARAKI, M. KONDO, *Biosci. Biotechnol. Biochem.* **2003**, *67*, 2269–2272.
[20] K. F. Wang, R. Nagarajan, T. A. Camesano, *Colloids Surf. B Biointerfaces* **2014**, *116*, 472–481.
[21] L. Stella, M. Burattini, C. Mazzuca, A. Palleschi, M. Venanzi, I. Coin, C. Peggion, C. Toniolo, B. Pispisa, *Chem. Biodivers.* **2007**, *4*, 1299–1312.
[22] J. Dittmer, L. Thogersen, J. Underhaug, K. Bertelsen, T. Vosegaard, J. M. Pedersen, B. Schiott, E. Tajkhorshid, T. Skrydstrup, N. C. Nielsen, *J. Phys. Chem. B* **2009**, *113*, 6928–6937.
[23] M. Eisenberg, J. E. Hall, C. A. Mead, *J. Membr. Biol.* **1973**, *14*, 143–176.
[24] J. Sikkema, J. A. de Bont, B. Poolman, *Microbiol. Rev.* **1995**, *59*, 201–222.
[25] J. Sikkema, J. A. de Bont, B. Poolman, *J. Biol. Chem.* **1994**, *269*, 8022–8028.
[26] J. C. Biffinger, H. W. Kim, S. G. DiMagno, *ChemBioChem* **2004**, *5*, 622–627.
[27] W. K. Hagmann, *J. Med. Chem.* **2008**, *51*, 4359–4369.
[28] B. C. Buer, E. N. G. Marsh, *Protein Sci.* **2012**, *21*, 453–462.
[29] J. Rivera-Chávez, H. A. Raja, T. N. Graf, J. E. Burdette, C. J. Pearce, N. H. Oberlies, *J. Nat. Prod.* **2017**, *80*, 1883–1892.
[30] M. Meldal, C. W. Tornoe, *Chem. Rev.* **2008**, *108*, 2952–3015.
[31] E. D. Goddard-Borger, R. V. Stick, *Org. Lett.* **2007**, *9*, 3797–3800.
[32] K. Ben Haj Salah, N. Inguimbert, *Org. Lett.* **2014**, *16*, 1783–1785.
[33] K. Ben Haj Salah, B. Legrand, S. Das, J. Martinez, N. Inguimbert, *Pept. Sci.* **2015**, *104*, 611–621.
[34] R. Subirós-Funosas, R. Prohens, R. Barbas, A. El-Faham, F. Albericio, *Chem. – Eur. J.* **2009**, *15*, 9394–9403.
[35] T. Degenkolb, A. Berg, W. Gams, B. Schlegel, U. Gräfe, *J. Pept. Sci.* **2003**, *9*, 666–678.
[36] A.-I. Van Bohemen, A. Zalouk-Vergnoux, L. Poirier, N. N. Phuong, N. Inguimbert, K. Ben Haj Salah, N. Ruiz, Y. F. Pouchus, *J. Chromatogr. B* **2016**, *1009*, 25–33.
[37] A. Psurek, C. Neusüß, T. Degenkolb, H. Brückner, E. Balaguer, D. Imhof, G. K. E. Scriba, *J. Pept. Sci.* **2006**, *12*, 279–290.
[38] A. Chakrabartty, T. Kortemme, S. Padmanabhan, R. L. Baldwin, *Biochemistry (Mosc.)* **1993**, *32*, 5560–5565.
[39] C. D. Andrew, S. Bhattacharjee, N. Kokkoni, J. D. Hirst, G. R. Jones, A. J. Doig, *J. Am. Chem. Soc.* **2002**, *124*, 12706–12714.
[40] V. R. Thalladi, H.-C. Weiss, D. Bläser, R. Boese, A. Nangia, G. R. Desiraju, *J. Am. Chem. Soc.* **1998**, *120*, 8702–8710.
[41] B. Legrand, C. André, E. Wenger, C. Didierjean, M. C. Averlant-Petit, J. Martinez, M. Calmes, M. Amblard, *Angew. Chem. Int. Ed.* **2012**, *51*, 11267–11270.
[42] L. Mathieu, B. Legrand, C. Deng, L. Vezenkov, E. Wenger, C. Didierjean, M. Amblard, M.-C. Averlant-Petit, N. Masurier, V. Lisowski, et al., *Angew. Chem. Int. Ed.* **2013**, *52*, 6006–6010.
[43] G. Esposito, J. A. Carver, J. Boyd, I. D. Campbell, *Biochemistry (Mosc.)* **1987**, *26*, 1043–1050.
[44] M. el Hajji, S. Rebuffat, T. Le Doan, G. Klein, M. Satre, B. Bodo, *Biochim. Biophys. Acta* **1989**, *978*, 97–104.
[45] A. S. Ladokhin, W. C. Wimley, S. H. White, *Biophys. J.* **1995**, *69*, 1964–1971.
[46] J. B. Birks, *Rep. Prog. Phys.* **1975**, *38*, 903.
[47] M. O. Guler, R. C. Claussen, S. I. Stupp, *J. Mater. Chem.* **2005**, *15*, 4507–4512.
[48] G. Bocchinfuso, S. Bobone, C. Mazzuca, A. Palleschi, L. Stella, *Cell. Mol. Life Sci.* **2011**, *68*, 2281–2301.

Entry for the Table of Contents (Please choose one layout)

FULL PAPER

Change the N-terminal tail. 4-aromatic substituted 1,2,3-triazoles can be used for replacing the N-acetyl capping of peptides. These moieties were easily synthesized and introduced by solid phase peptide synthesis on antimicrobial peptaibols increasing their biological activity up to eight times without modification of overall three-dimensional structure.

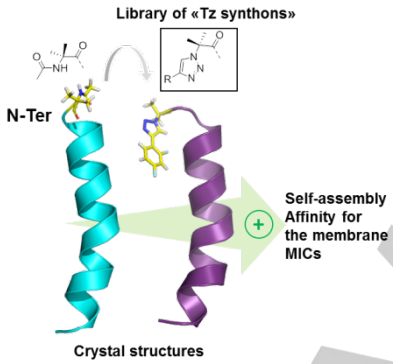

*S. Das, K. Ben Haj Salah, E. Wenger, J. Martinez, J. Kotarba, V. Andreu, N. Ruiz, F. Savini, L. Stella, C. Didierjean, B. Legrand and N.Inguimbert**

Page No. – Page No.

Enhancing the antimicrobial activity of alamethicin F50/5 by incorporating N-terminal hydrophobic triazole substituents.